

## Supporting Information

### **Composites of Azo-Linked Pyrene-Tetraone Porous Organic Polymers as Cathodes for Lithium-ion Batteries**

Heba H. Farrag<sup>1,2</sup>, Eloi Grignon<sup>1</sup>, Alicia M. Battaglia<sup>1</sup>, Jiang Tian Liu<sup>1</sup>, and Dwight S. Seferos<sup>1,3\*</sup>

<sup>1</sup>Department of Chemistry, University of Toronto, Lash Miller Chemical Laboratories, 80 St. George Street, Toronto, Ontario, M5S 3H6, Canada

<sup>2</sup>Department of Chemistry, Faculty of Science, Cairo University, Cairo 12613, Egypt

<sup>3</sup>Department of Chemical Engineering and Applied Chemistry, University of Toronto, 200 College Street, Toronto, Ontario, M5S 3E5, Canada

*\*Corresponding authors. Email address: [dwight.seferos@utoronto.ca](mailto:dwight.seferos@utoronto.ca)*

## Table of Contents

1. Experimental Section.....	S4
1.1 Materials.....	S4
1.2 Instrumentation.....	S4
1.3 Synthetic Procedures.....	S6
1.4 Electrode Preparation.....	S10
1.5 Coin Cell Assembly.....	S11
2. Physical Characterization.....	S11
3. Electrode and Electrochemical characterization.....	S21
4. References.....	S29

## List of Figures and Tables

<b>Figure S1.</b> $^1\text{H}$ NMR (400 MHz, DMSO- $d_6$ ) spectrum of PTO.....	S12
<b>Figure S2.</b> $^{13}\text{C}$ NMR (125 MHz, DMSO- $d_6$ ) spectrum of PTO.....	S13
<b>Figure S3.</b> $^1\text{H}$ NMR (400 MHz, DMSO- $d_6$ ) spectrum of DNPTO.....	S13
<b>Figure S4.</b> $^{13}\text{C}$ NMR (125 MHz, DMSO- $d_6$ ) spectrum of DNPTO.....	S14
<b>Figure S5.</b> $^1\text{H}$ NMR (400 MHz, DMSO- $d_6$ ) spectrum of DAPTO.....	S14
<b>Figure S6.</b> $^{13}\text{C}$ NMR (125 MHz, DMSO- $d_6$ ) spectrum of DAPTO.....	S15
<b>Figure S7.</b> $^{13}\text{C}$ solid state NMR CP/MAS spectrum of Azo-PTP.....	S16
<b>Figure S8.</b> $^1\text{H}$ NMR (400 MHz, DMSO- $d_6$ ) spectrum of the DAPTO homocoupling product...	S17
<b>Figure S9.</b> FTIR spectra of TAPA (black) and the TAPA homocoupling product (TAPA-H, pink).....	S18
<b>Figure S10.</b> (A) XPS survey spectrum, Deconvoluted XPS (B) N 1s, (C) O 1s spectra of Azo-PTP.....	S19

**Figure S11.** FTIR spectra of (A) Azo-PTP30 (blue), and Azo-PTP50 (purple), (B) zoom in spectra of Azo-PTP50 to detect the carbonyl and the azo peaks.....S20

**Figure S12.** SEM images of (A) Azo-PTP, (B) Azo-PTP30, and Azo-PTP50 as solid .....S21

**Figure S13.** Solubility test conducted on the pristine Azo-PTP composite film within a 1 M LiTFSI electrolyte, featuring a 1:1 (v/v) ratio of 1,3-dioxolane to dimethoxyethane.....S22

**Figure S14.** The theoretical capacity of Azo-PTP at different potential window.....S22

**Figure S15.** Chemical structure of Azo-PTP indicating the TAPA unit and PTO unit.....S24

**Figure S16.** (A) Rate capability, (B) cycling stability at 100 mA g<sup>-1</sup>, and (C) galvanostatic charge/discharge at 50 mA g<sup>-1</sup> of Azo-PTP, Azo-PTP30, and Azo-PTP50 at 1.0 – 3.5 V.....S25

**Figure S17.** (A) Galvanostatic charge/discharge curve of CNT electrode at 50 mA g<sup>-1</sup>, (B) Rate performance of CNT electrode at 1.0 to 3.5 V.....S26

**Figure S18:** Differential capacity plots for cycle 8 of Azo-PTP (red), Azo-PTP30 (blue), and Azo-PTP50 (purple).....S26

**Figure S19:** (A) Galvanostatic charge/discharge curve of CNT electrode at 50 mA g<sup>-1</sup>, (B) Rate performance of CNT electrode at 1.5 – 3.5 V.....S27

**Figure S20:** Rate capability of Azo-PTP50 electrode with two different compositions: 80:10:10 (active material: super P: PVDF, pink) and 60:30:10 (purple).....S28

**Figure S21:** Nyquist plots of the polymers at open-circuit voltage after ten activation cycles....S29

**Table S1:** The mass loading details for electrodes prepared with Azo-PTP, Azo-PTP30, and Azo-PTP50.....S1  
1

**Table S2:** Summary of the specific capacity of each prepared electrodes at different current density at 1.0 – 3.5 V.....S30

**Table S3:** Summary of the specific capacity of each prepared electrodes at different current density at 1.5 – 3.5 V.....S30

**Table S4:** Comparison of the electrochemical performance of the prepared polymers with other organic cathodes featuring carbonyl and/or azo groups as redox-active units, as reported in the literature.....S31

## **1. Experimental Section**

### **1.1 Materials**

Pyrene ( $\geq 99\%$ ), sodium periodate ( $\geq 99.8\%$ ), ruthenium (III) chloride hydrate ( $\geq 99.9\%$ ), dichloromethane (DCM), sodium bicarbonate ( $\geq 99.7\%$ ), sodium hydrosulfite, sodium hydroxide ( $\geq 97\%$ ), ammonium chloride ( $\geq 99.5\%$ ), 2,3-dichloro-5,6-dicyano-p-benzoquinone (DDQ), methanol, copper (I) bromide (99.9%), pyridine ( $\geq 99\%$ ), hydrochloric acid (37%), dimethyl sulfoxide (DMSO) (anhydrous,  $\geq 99.9\%$ ), toluene ( $\geq 99.5\%$ ), dimethylformamide (DMF), poly(vinylidene fluoride) (PVDF), 1,3-dioxolane (anhydrous,  $\geq 99.8$ ), and 1,2-dimethoxyethane (anhydrous, 99.5%) were purchased from Sigma-Aldrich and used as received. Fuming nitric acid (98%), sulfuric acid (reagent grade), tris(4-aminophenyl) amine (TAPA) were purchased from Fisher Scientific. All other solvents were purchased from Sigma-Aldrich and used as received.

### **1.2 Instrumentation**

Solution NMR spectra were acquired at room temperature employing either a 400 MHz Bruker Advance III or a 600 MHz Agilent DD2 NMR spectrometer, with referencing to the residual DMSO peak. For solid-state cross polarization magic angle spinning (CP-MAS) NMR spectra, a

700 MHz Agilent DD2 NMR spectrometer was utilized, with adamantane serving as the reference compound. Fourier transform infrared (FTIR) measurements were conducted using a Thermo Scientific iS50 instrument. Raman measurements were performed employing a Bruker SENTERRA Dispersive Raman Microscope. Mass spectra was recorded on a JEOL AccuTOF Plus 5G model JMS-T1000LP mass spectrometer equipped with a Direct Analysis in Real Time (DART) ion source.

Nitrogen adsorption–desorption isotherm analysis was performed using an Autosorb iQ of Quantachrome Instruments. The samples were degassed under vacuum at 40 °C for 1000 mins before each measurement. The specific surface area was calculated using the Brunauer–Emmett–Teller (BET) method at relative pressures of  $0.05 < p/p_0 < 0.3$ .

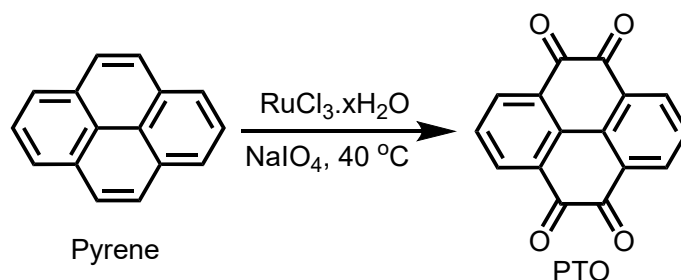
Thermogravimetric analysis (TGA) measurements were performed using a Netzsch STA 449 F3 Jupiter instrument under an argon atmosphere with a flow rate of 50 mL min<sup>-1</sup> and a heating rate of 10 °C min<sup>-1</sup>. Powder X-ray diffraction (pXRD) patterns were obtained using a Rigaku MiniFlex 600 6G Benchtop X-ray diffractometer instrument equipped with Cu K $\alpha$  radiation ( $\lambda = 1.5406$  Å). The X-ray photoelectron spectroscopy (XPS) spectrum was recorded using a Thermo Scientific K-Alpha spectrometer featuring a monochromatic Al K $\alpha$  source. Scanning electron microscopy (SEM) analysis was conducted on a Quanta 250 FEG Environmental SEM instrument operating at an accelerating voltage of 5 kV.

Battery capacities and rates were computed considering the active material weight percentage in the cathode. The electrochemical performance of the batteries was evaluated using a Neware BTS4000 battery testing system at room temperature. Cyclic voltammetry (CV) measurements were conducted utilizing a Bio-Logic BCS-805 battery tester equipped with a frequency response analyzer. Impedance measurements were taken from 10 kHz to 100 mHz at open circuit voltage

with a potential perturbation of 10 mV. Prior to the measurements, the cells were cycled ten times at 50 mA/g and then rested for 10 hours.

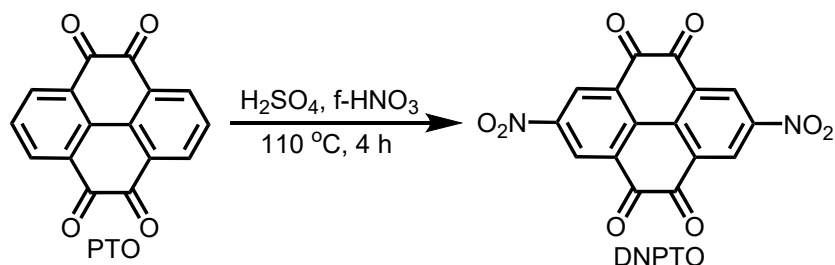
### 1.3 Synthetic Procedures

#### Synthesis of pyrene-4,5,9,10-tetraone (PTO)



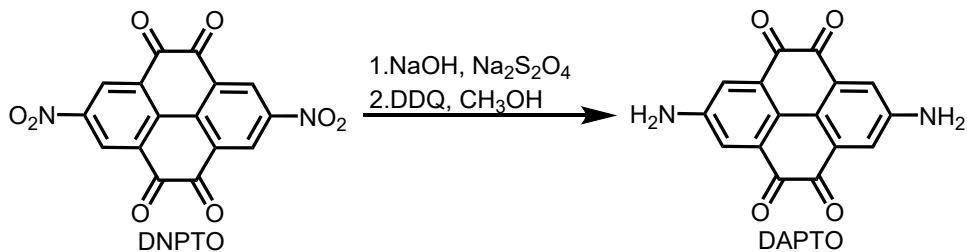
PTO was synthesized using a previously reported method with slight modifications.<sup>1,2</sup> Pyrene (4 g, 20 mmol) was dissolved in a combined solution of dichloromethane (80 mL) and acetonitrile (80 mL). Subsequently, sodium periodate (35.0 g, 164 mmol),  $\text{H}_2\text{O}$  (100 mL), and ruthenium (III) chloride hydrate (0.5 g, 0.42 mmol) were introduced into the mixture. The reaction proceeded with stirring at  $40\text{ }^\circ\text{C}$  overnight. Following the reaction, the suspension was separated through vacuum filtration, and the resulting precipitate was thoroughly washed with abundant amounts of DCM producing orange solution. The evaporation of this solution using rotary evaporation yielded an orange solid (1.3 g, 25% yield) of PTO without the need for additional purification.  $^1\text{H}$  NMR (400 MHz,  $\text{DMSO}-d_6$ )  $\delta$  8.33 (d,  $J = 7.7\text{ Hz}$ , 4H), 7.74 (t,  $J = 7.7\text{ Hz}$ , 2H).  $^{13}\text{C}$  NMR (125 MHz,  $\text{DMSO}-d_6$ ,  $\delta$  ppm): 177.5, 134.5, 134.1, 131.9, 130.6. HRMS (DART-TOF)<sup>+</sup>  $m/z$ : calculated for  $[\text{C}_{16}\text{H}_6\text{O}_4]$   $[\text{M}+\text{NH}_4]^+$ : 280.22, found: 280.06.

### Synthesis of 2,7-dinitropyrene-4,5,9,10-tetraone (DNPTO)



DNPTO was synthesized following a modified version of the reported protocol.<sup>3</sup> PTO (524 mg, 2 mmol) was combined with a (20 mL) mixture of concentrated sulfuric acid and fuming nitric acid (4:1, v/v) and heated at  $110\text{ }^\circ\text{C}$  for four hours. After cooling to room temperature, the reaction mixture was poured into (200 mL) of ice water. Neutralization was achieved by the addition of saturated  $\text{NaHCO}_3$  solution. The resulting yellow precipitate was collected by vacuum filtration and washed with water multiple times. The solid was then dried under vacuum at  $70\text{ }^\circ\text{C}$  for 24 hours, yielding 453.9 mg of DNPTO as a yellow powder with a 64% yield.  $^1\text{H}$  NMR (400 MHz,  $\text{DMSO-d}_6$ )  $\delta$  8.90 (s, 4H).  $^{13}\text{C}$  NMR (125 MHz,  $\text{DMSO-d}_6$ )  $\delta$  174.61, 149.09, 136.23, 134.46, 126.36. HRMS (DART-TOF)<sup>+</sup>  $m/z$ : calculated for  $[\text{C}_{16}\text{H}_4\text{N}_2\text{O}_8]$   $[\text{M}+\text{Li}]^+$ : 355.21, found: 355.0.

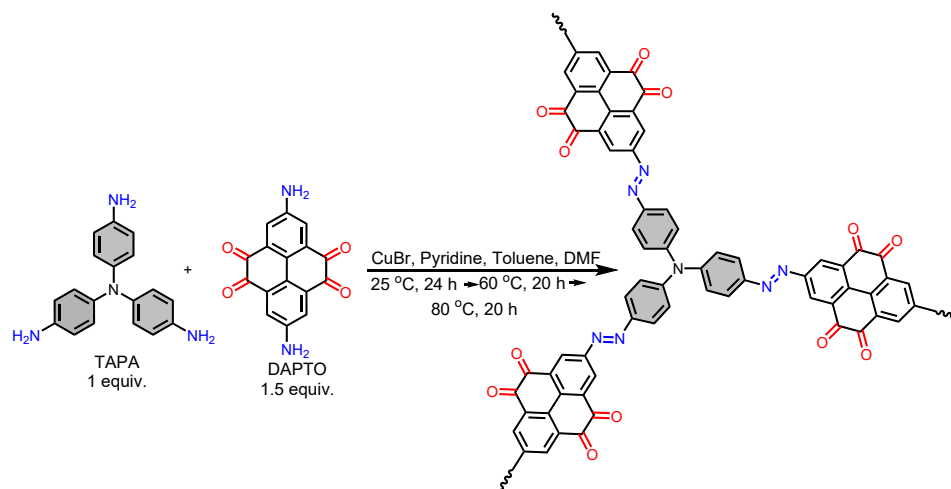
### Synthesis of 2,7-diaminopyrene-4,5,9,10-tetraone (DAPTO)



The synthesis of DAPTO was conducted following a literature procedure with some adaptations.<sup>4</sup> In a round flask containing sodium hydroxide (4.45 g, 112 mmol), water (75 mL), and sodium hydrosulfite (2.2 g, 12.75 mmol), DNPTO (0.5 g, 1.4 mmol) was introduced, and the reaction was

heated to 50 °C for 30 minutes. Subsequently, the reaction mixture was poured into a solution of saturated ammonium chloride (250 mL). The resulting suspension was filtered, and the filtrate was washed with water to yield a black powder. This material was then dried under vacuum at room temperature overnight to obtain the crude product. The crude product (242.5 mg), 2,3-dichloro-5,6-dicyano-p-benzoquinone (796 mg, 3.5 mmol), and methanol (16 mL) were stirred at 35 °C overnight. Following this, the reaction solution was diluted by the addition of ethyl acetate (30 mL). The suspension was separated through centrifugation and washed with ethyl acetate several times, resulting in the formation of 165 mg of DAPTO as a black solid, achieving a 50% yield. <sup>1</sup>H NMR (400 MHz, DMSO-d<sub>6</sub>) δ 7.36 (s, 4H), 5.95 (s, 4H). <sup>13</sup>C NMR (125 MHz, DMSO-d<sub>6</sub>) δ 119.29, 124.83, 131.23, 148.93, and 178.84. HRMS (DART-TOF)<sup>+</sup> *m/z*: calculated for [C<sub>16</sub>H<sub>10</sub>N<sub>2</sub>O<sub>4</sub>]<sup>+</sup> 294.27, found: 293.1.

### Synthesis of azo-linked pyrenetetraone two-dimensional porous polymer (Azo-PTP)

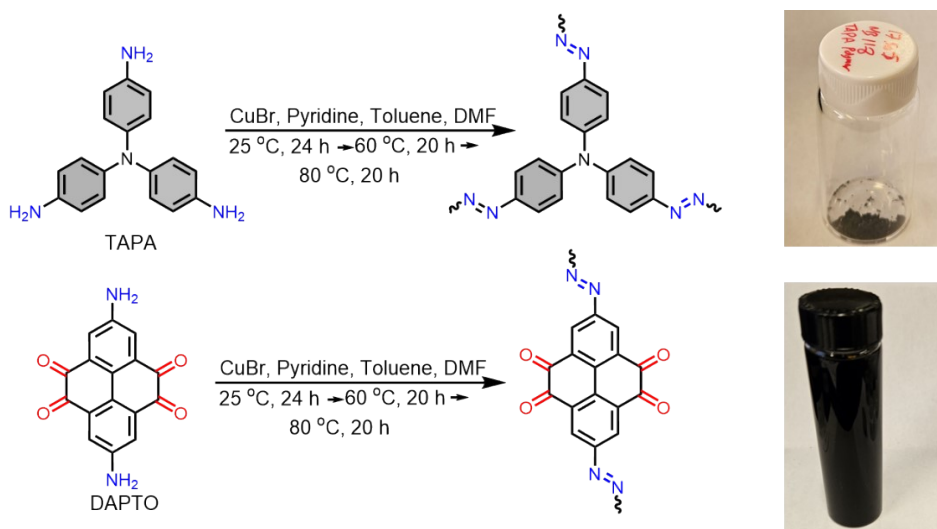


The synthesis method for Azo-PTP was adapted from previously reported literature.<sup>5,6</sup> In a 100 mL round-bottom flask, a solution of CuBr (40 mg, 0.279 mmol) and pyridine (160 mg, 2.02 mmol) in toluene (11 mL) was stirred for 3 hours at room temperature, resulting in a homogeneous mixture (**designated as Mixture 1**). In a separate flask, tris(4-aminophenyl) amine (TAPA) (40



mg, 0.138 mmol) and DAPTO (60.2 mg, 0.206 mmol) were combined in DMF (11 mL) and sonicated for 30 minutes to achieve homogeneity (**designated as Mixture 2**). **Mixture 2** was then carefully added dropwise to **Mixture 1**. The resulting suspension was stirred consecutively at 25 °C for 24 hours, 60 °C for 20 hours, and 80 °C for an additional 20 hours. Subsequently, the formed black precipitate was isolated by vacuum filtration, followed by thorough washing with DMF and water. The resulting solid was further stirred in a 100 mL HCl solution (2M) overnight. The resultant black solid was once again collected via filtration and washed successively with 2M NaOH, water, dimethyl sulfoxide (DMSO), DMF, and acetone. The resulting solid was then dried and subjected to Soxhlet extraction with methanol for 24 hours. The purified solid was collected and vacuum-dried at 120 °C overnight, yielding 60 mg of Azo-PTP as a black solid with a 60% yield.

### Synthesis of DAPTO and TAPA Homopolymers as References for Azo-PTP



For the synthesis of the DAPTO homopolymer, DAPTO (100.6 mg, 0.344 mmol) was dissolved in DMF (11 mL) and stirred under the same conditions as for Azo-PTP synthesis. After filtration, the resulting product was found to be soluble in DMF, so the purification process was stopped

after this step. In contrast, for the TAPA homopolymer, TAPA (100 mg, 0.344 mmol) was dissolved in DMF (11 mL) and subjected to the same reaction and purification steps as Azo-PTP, yielding the TAPA homopolymer. These homopolymers were synthesized to assess the possibility of homocoupling and provide a reference for the Azo-PTP structure and performance.

### **Synthesis of Azo-PTP@CNTs composites**

The synthesis of Azo-PTP with CNTs composites closely mirrored the procedure for synthesizing Azo-PTP without CNTs. The key difference occurred during the preparation of **Mixture 2**, where carbon nanotubes (CNTs) were introduced. Specifically, CNTs were incorporated into the combination of TAPA and DAPTO in DMF. The mixture was subjected to sonication for 30 minutes, resulting in **Mixture 2**. Different amounts of CNTs were used, specifically 30% (Azo-PTP30) and 50% (Azo-PTP50) by weight, calculated based on the expected yield of Azo-PTP as indicated in similar studies.<sup>4</sup> For clarity, the synthesis of Azo-PTP consistently yielded 60 mg of product, as previously mentioned. Therefore, for the synthesis of Azo-PTP30 and Azo-PTP50 with 30 and 50 wt. % of CNTs, 26 mg and 60 mg of CNTs, respectively, were added to the reaction mixture to prepare the composites. This modification aimed to explore the impact of different CNT concentrations on the composite's properties and performance. The overall synthetic procedure remained consistent with that of Azo-PTP alone, ensuring a systematic comparison between the composite and the pristine material.

### **1.4 Electrode preparation**

The cathode electrodes were prepared according to the following procedure: PVDF was stirred in N-methyl-2-pyrrolidone (NMP) in a small vial equipped with a stir bar until completely dissolved. The active material (Azo-PTP, Azo-PTP30, or Azo-PTP50) was then added and stirred for 15

minutes. Subsequently, Super P was added and stirred for another 15 minutes to form a slurry with a concentration of 125 mg/mL. The slurries were stirred over night and then sonicated for 6 hours, with stirring every one hour to ensure homogeneity. The mass ratio of active materials, carbon black, and PVDF was maintained at 60:30:10. The slurries were cast onto an aluminum foil current collector (15  $\mu\text{m}$  thickness) using a notch bar with a height of 200  $\mu\text{m}$ . The cast electrodes were air-dried on a hot plate at 120  $^{\circ}\text{C}$ , followed by overnight drying in a vacuum antechamber at 80  $^{\circ}\text{C}$ . The active mass loadings of the electrodes ranged from 0.2 to 0.25  $\text{mg}/\text{cm}^2$ , with detailed values provided in **Table S1**. These loadings were applied over a geometric surface area of 2  $\text{cm}^2$ .

**Table S1:** The mass loading details for electrodes prepared with Azo-PTP, Azo-PTP30, and Azo-PTP50.

Electrodes	Mass loading $\text{mg}/\text{cm}^2$		
	*All additives	(polymer + CNTs)	Active material (polymer)
<b>Azo-PTP</b>	0.415	-----	0.25
<b>Azo-PTP30</b>	0.525	0.315	0.22
<b>Azo-PTP50</b>	0.665	0.399	0.2

\*All additives include the polymer, super P, and CNTs in case of Azo-PTP30 and Azo-PTP50.

The mass of the active material (AM) was calculated based on the following equation:

Mass of AM = mass of the film \* 0.6 (the percent of the AM in the film excluding the super P and PVDF) \* X (the percent of the AM excluding the percent of CNT). For Azo-PTP30, the X = 0.7 and for Azo-PTP50, the X = 0.5.

### 1.5 Coin cell assembly

CR2025-type coin cells (MTI Corporation) were assembled in an argon-filled glovebox. Electrodes were cut from the film using a 16 mm electrode punch (DPM Solutions Inc.). Lithium foil (0.38 mm thickness; 16 mm diameter), copper foil (25  $\mu\text{m}$  thickness, 16 mm diameter), and polypropylene separator (Celgard; 19 mm diameter) were utilized as the counter electrode, current collector, and separator, respectively. The electrolyte consisted of 80  $\mu\text{L}$  of 1 M lithium bis(trifluoromethanesulfonyl)imide (LiTFSI) in a 1:1 v/v mixture of 1,3-dioxolane and dimethoxy ethane (DME). A stainless-steel spacer (0.2 mm thickness) and a spring were included, and the cell was compressed using a digital pressure-controlled electric crimper (MTI Corporation). Prior to analysis, cells were allowed to rest for 18 hours at room temperature to ensure adequate permeation of the electrolyte into the electrodes. Given our focus on the material-specific electrochemical properties of the Azo-PTP, all capacities are normalized to the mass of the active material.

## **2. Physical characterization**

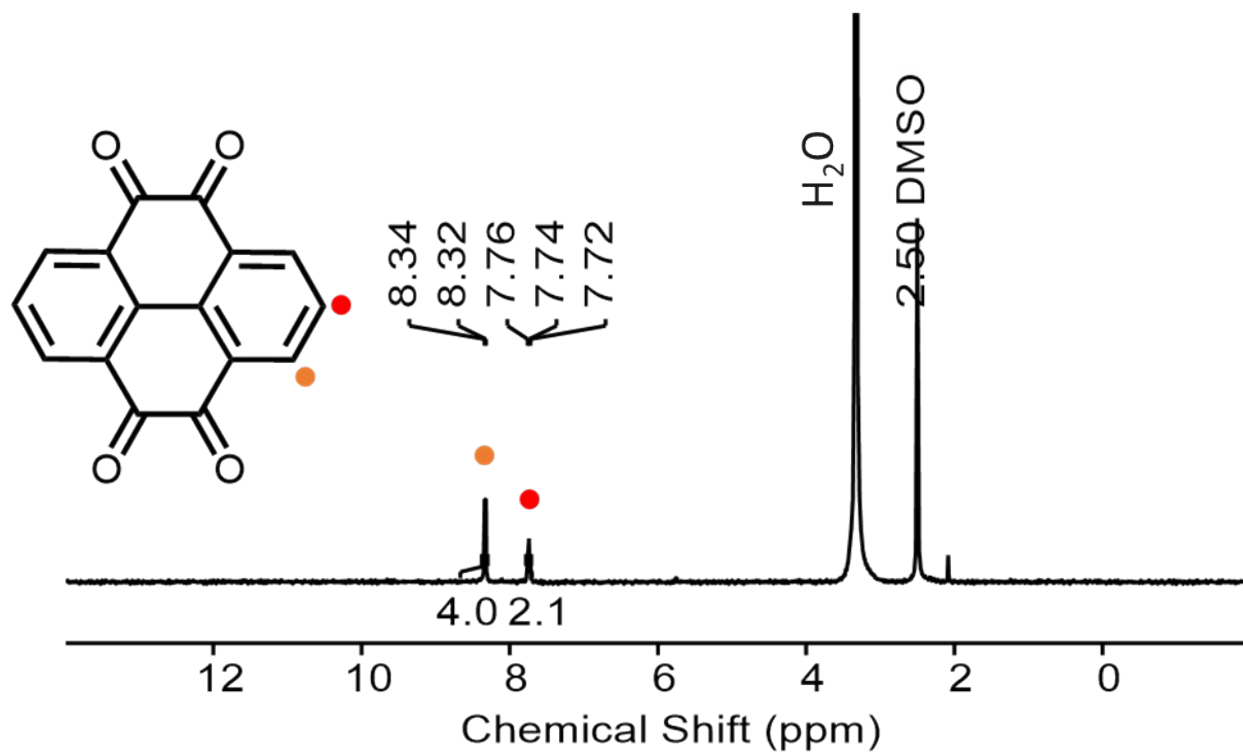


**Figure S1:**  $^1\text{H}$  NMR (400 MHz, DMSO- $d_6$ ) spectrum of PTO.

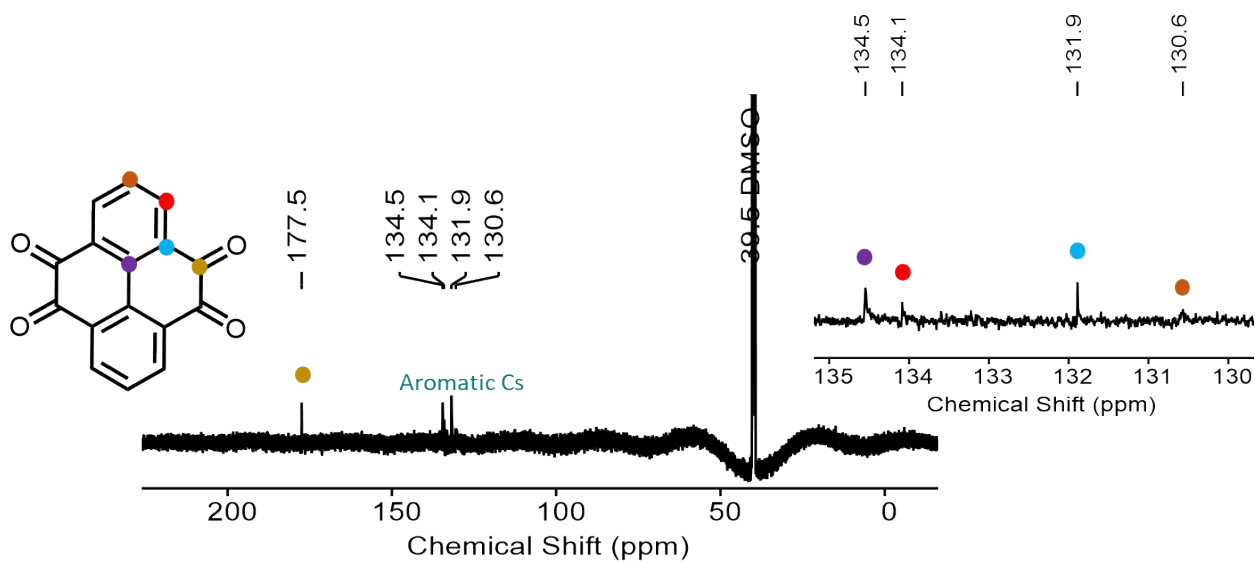


**Figure S2:**  $^{13}\text{C}$  NMR (125 MHz, DMSO- $d_6$ ) spectrum of PTO.

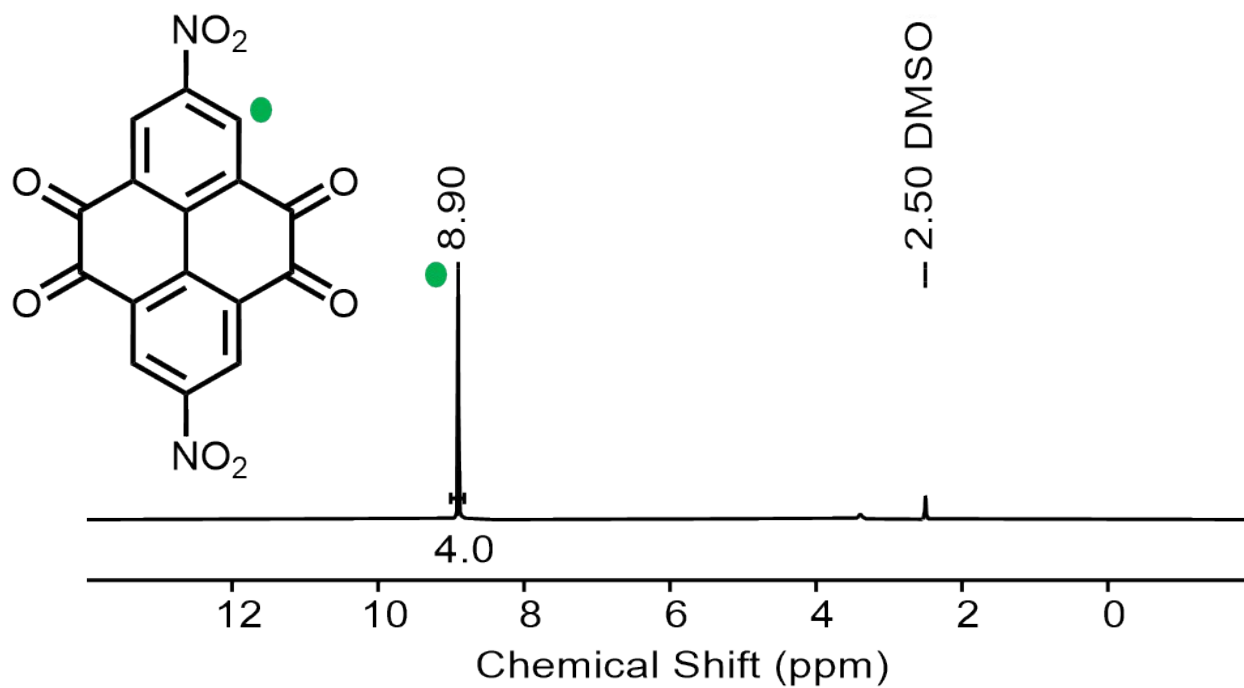


**Figure S3:**  $^1\text{H}$  NMR (400 MHz, DMSO- $d_6$ ) spectrum of DNPTO.

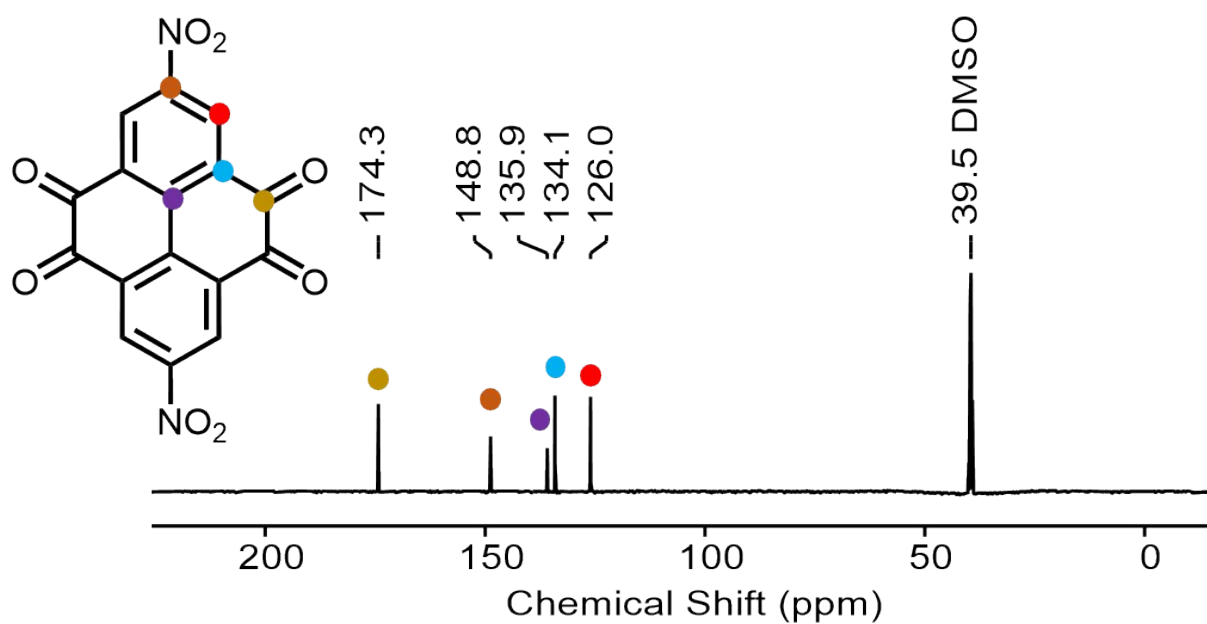


**Figure S4:**  $^{13}\text{C}$  NMR (125 MHz, DMSO- $d_6$ ) spectrum of DNPTO.



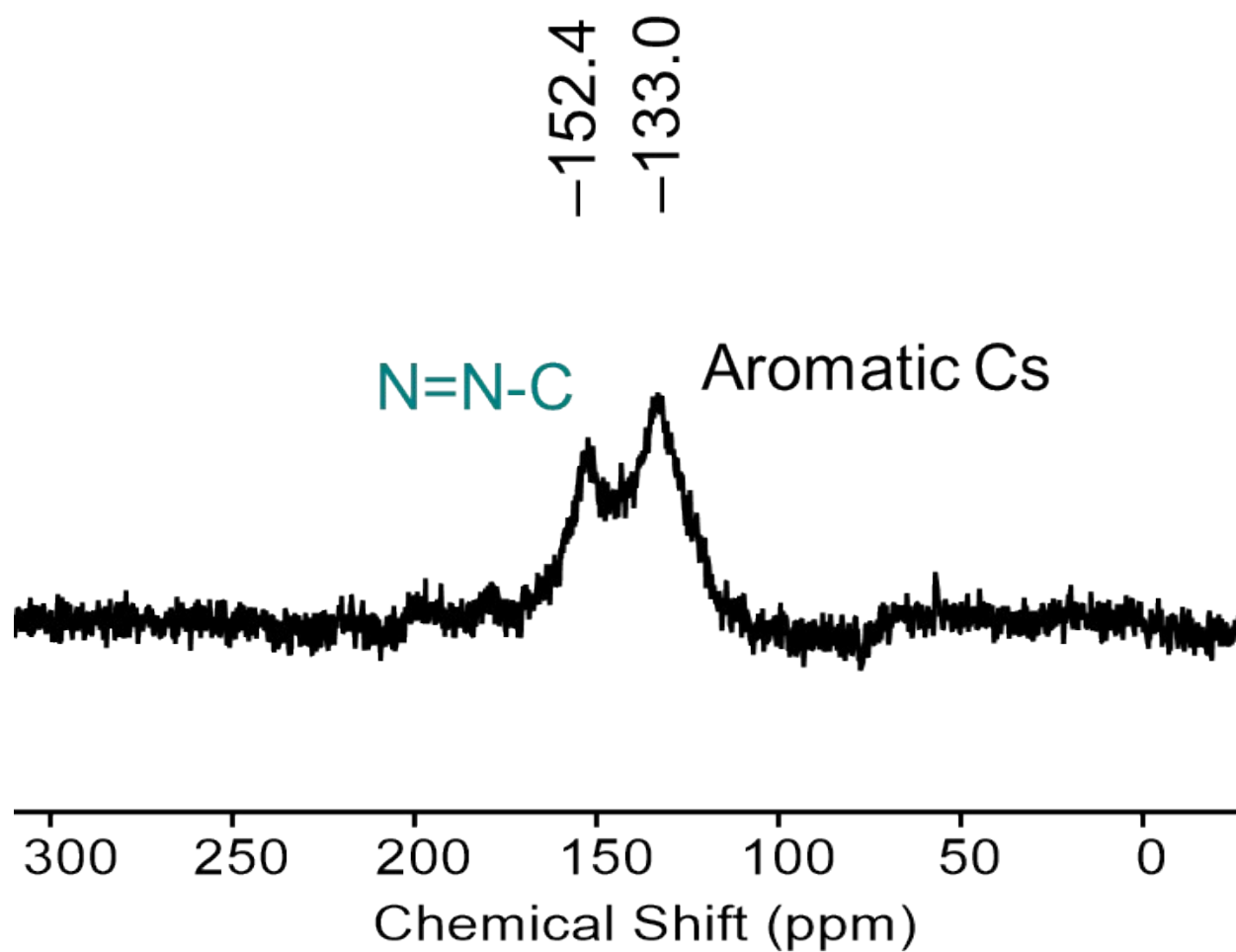


**Figure S7:**  $^{13}\text{C}$  solid state NMR CP/MAS spectrum of Azo-PTP.



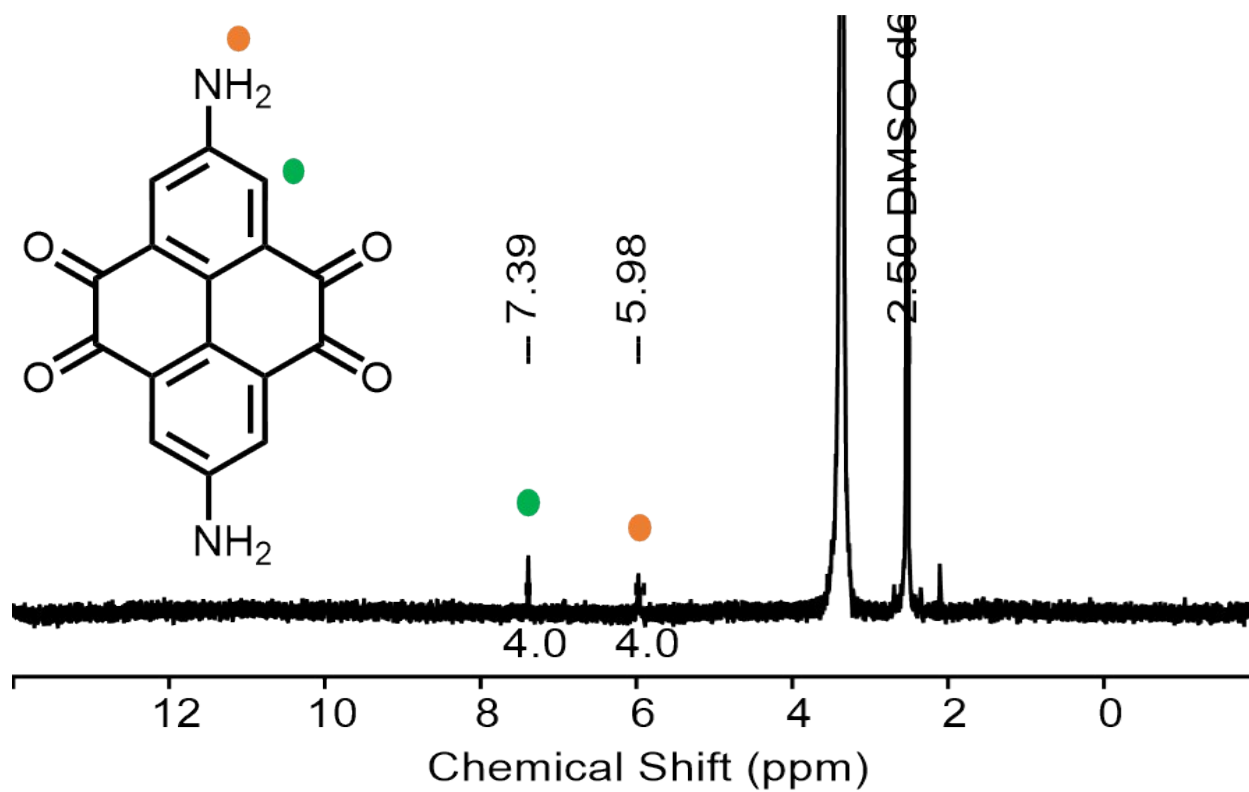


**Figure S8:**  $^1\text{H}$  NMR (400 MHz,  $\text{DMSO-d}_6$ ) spectrum of the DAPTO homocoupling product.

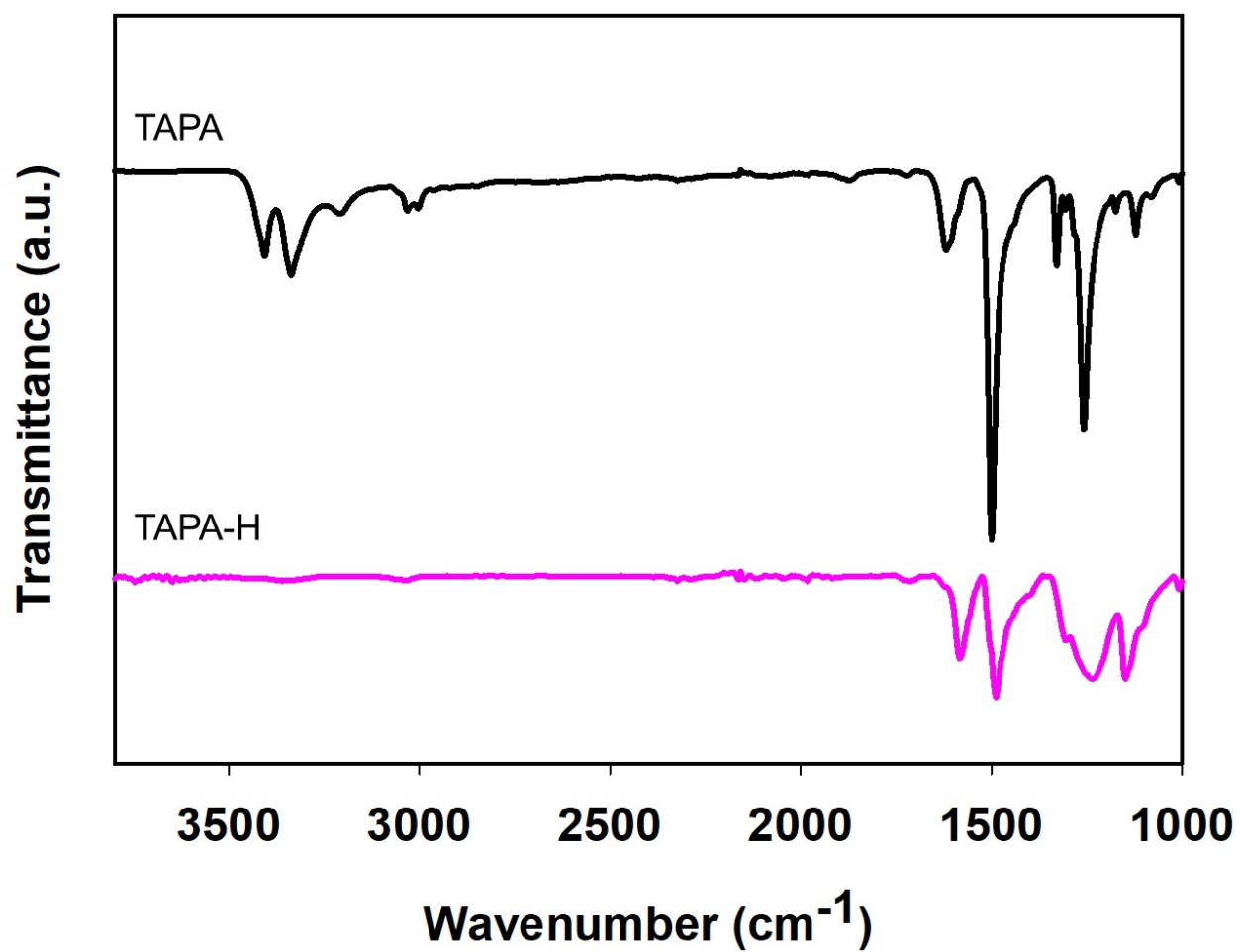


**Figure S9:** FTIR spectra of TAPA (black) and the TAPA homocoupling product (TAPA-H, pink).

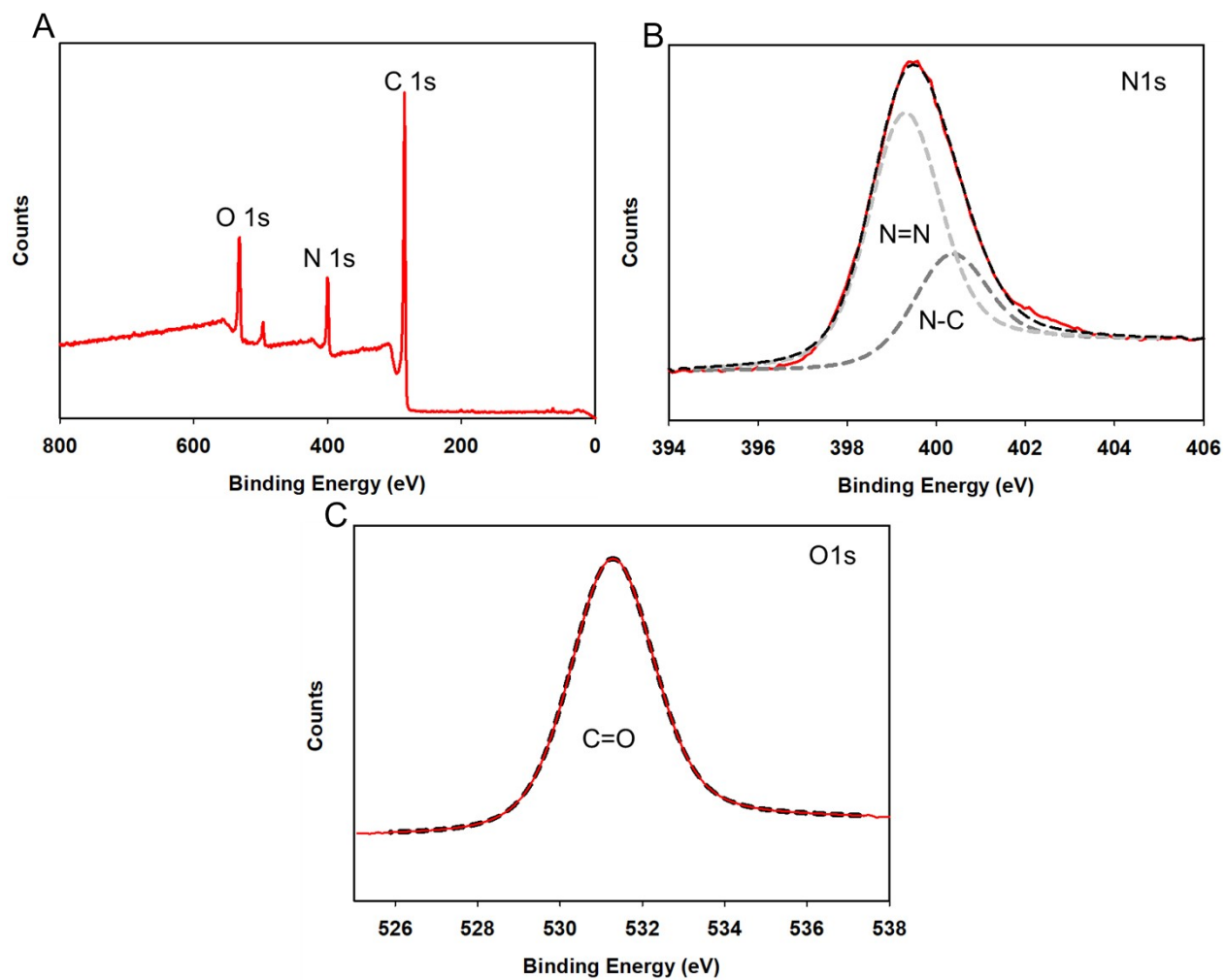


**Figure S10:** (A) XPS survey spectrum, Deconvoluted XPS (B) N 1s, (C) O 1s spectra of Azo-PTP.

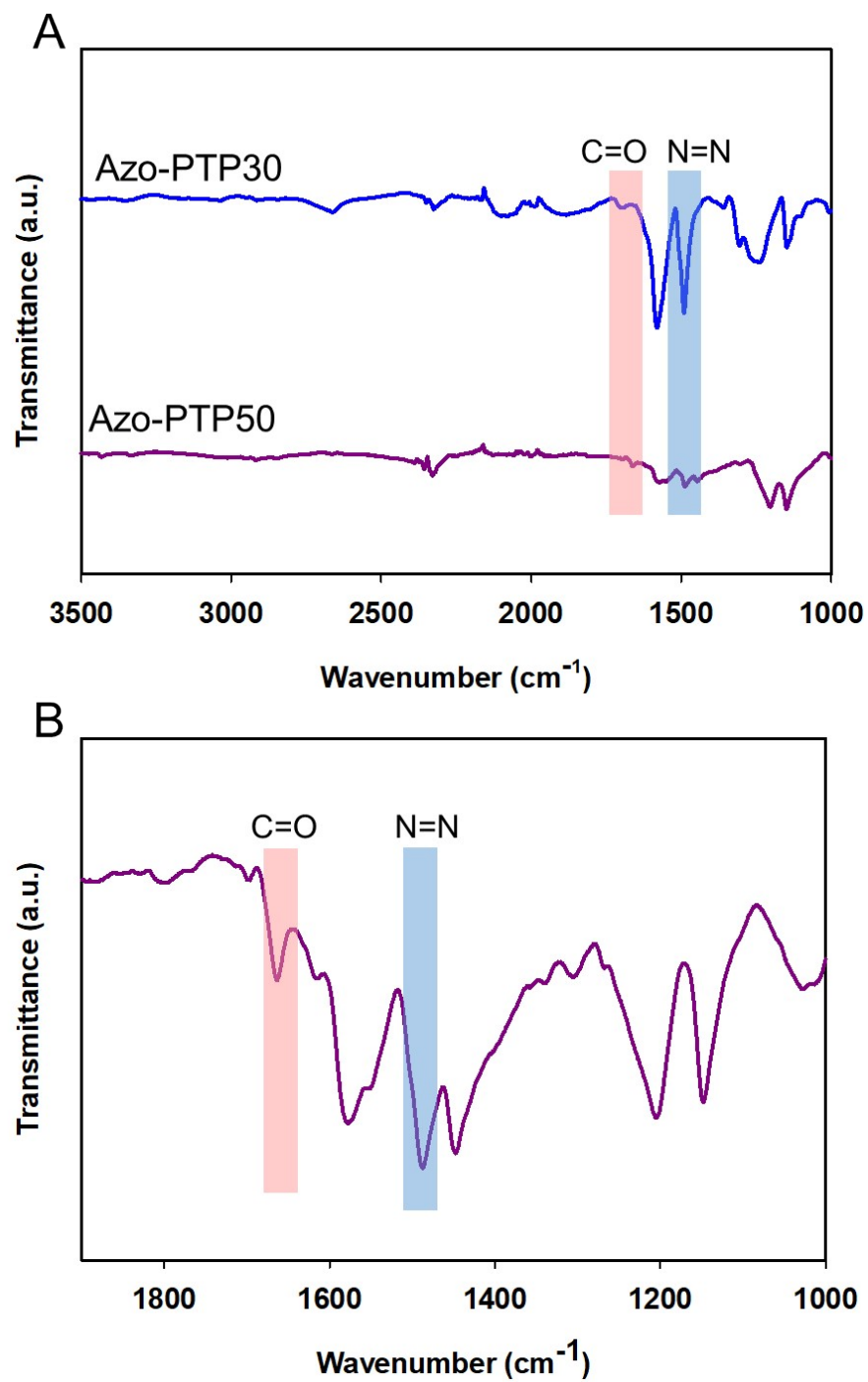


**Figure S11:** FTIR spectra of (A) Azo-PTP30 (blue), and Azo-PTP50 (purple), (B) zoom in spectra of Azo-PTP50 to detect the carbonyl and the azo peaks.

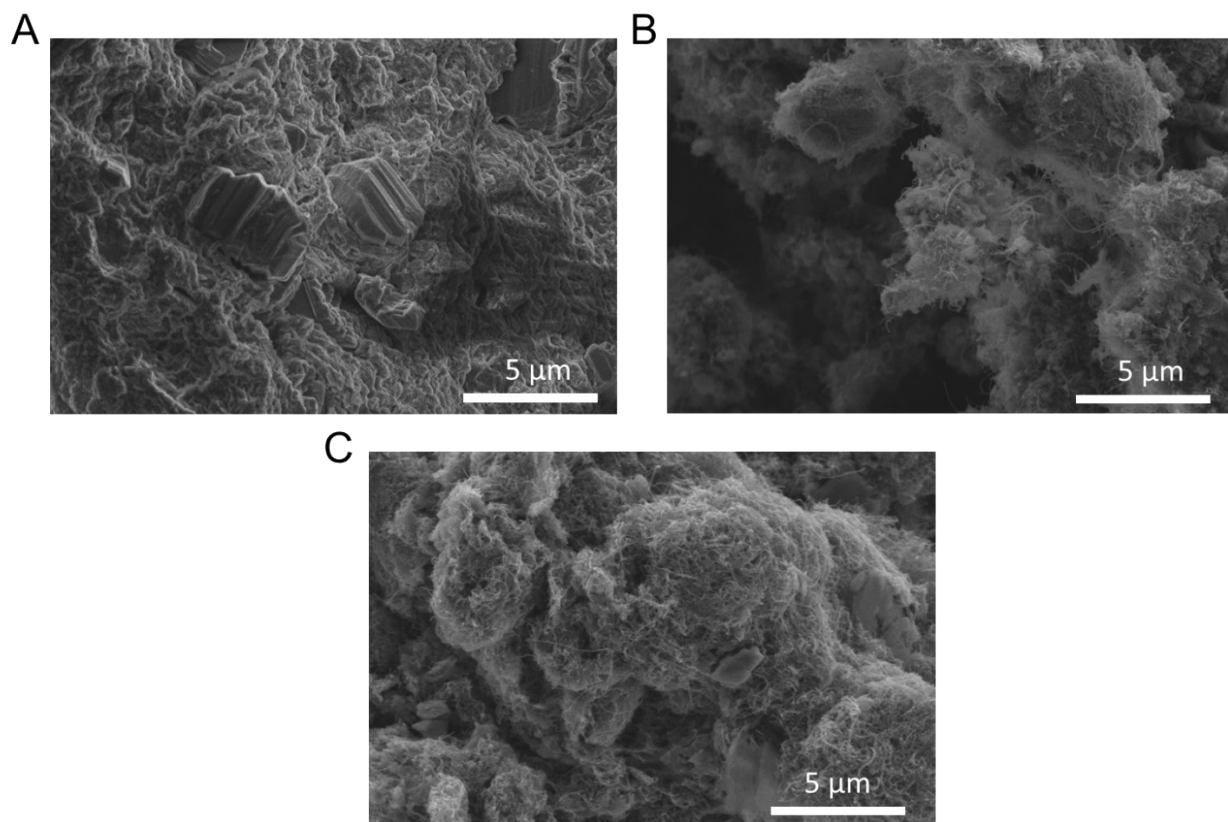


**Figure S12:** SEM images of (A) Azo-PTP, (B) Azo-PTP30, and Azo-PTP50 as solid.

### 3. Electrode and electrochemical characterization

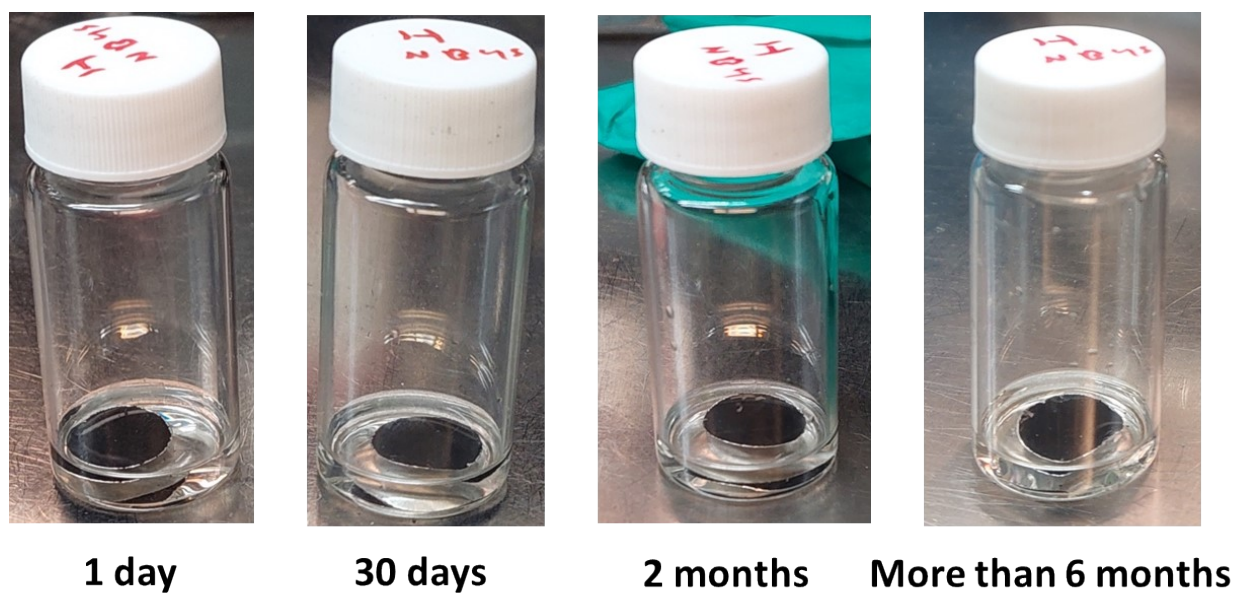


**Figure S13:** Solubility test conducted on the pristine Azo-PTP composite film within a 1 M LiTFSI electrolyte, featuring a 1:1 (v/v) ratio of 1,3-dioxolane to dimethoxyethane.

#### Theoretical capacity calculation

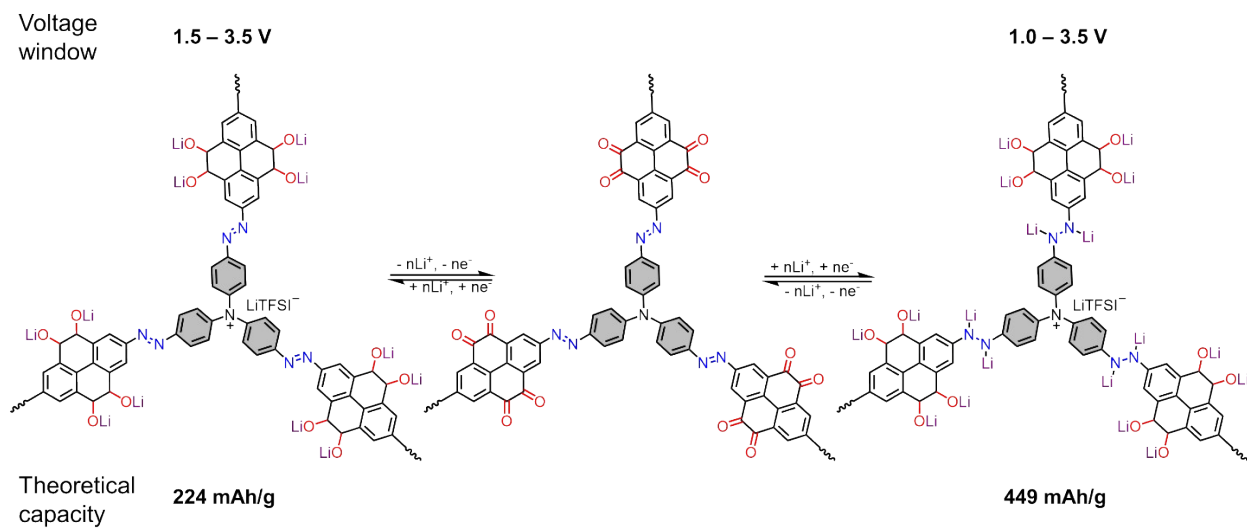


**Figure S14:** The theoretical capacity of Azo-PTP at different potential window.

The theoretical capacity ( $C_{th}$ ) was calculated based on the following equation:

$$C_{th} = \frac{n F}{3.6 M_w} \quad S1$$

In this equation,  $n$  denotes the number of electrons transferred per redox reaction,  $F$  is the Faraday constant ( $\sim 96,500 \text{ C mol}^{-1}$ ), and  $M_w$  represents the molecular weight of the repeating unit of the organic material. The molecular weights of the pyrenetetraone (PTO) and tris(4-aminophenyl)amine (TAPA) units in Azo-PTP are  $288 \text{ g mol}^{-1}$  and  $284 \text{ g mol}^{-1}$  (**Figure S2**), respectively. The repeating unit in Azo-PTP consists of half a PTO unit and one-third of a TAPA unit, resulting in a total molecular weight of  $238.67 \text{ g mol}^{-1}$  for the repeating unit cell. The number of electrons involved per repeating unit is 2 when the potential range is 1.5 to 3.5 V, yielding a theoretical capacity of 224 mAh/g. Expanding the potential window to 1.0 to 3.5 V enables the azo group to participate in the redox reaction, increasing the number of electrons to 4 and boosting the theoretical capacity to 449 mAh/g.

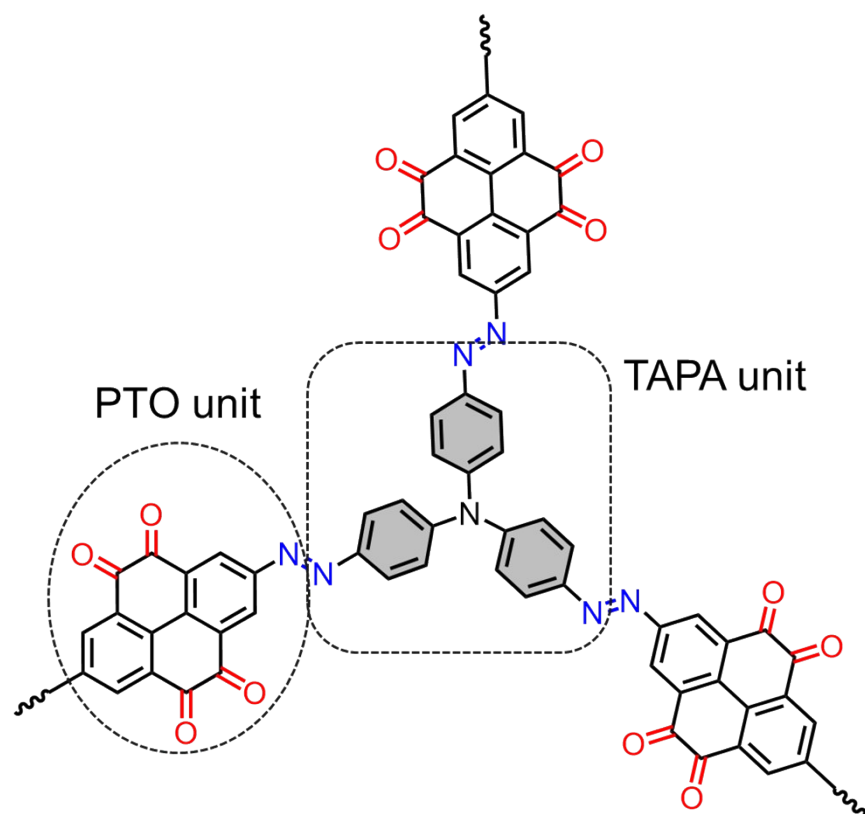


**Figure S15:** Chemical structure of Azo-PTP indicating the TAPA unit and PTO unit.



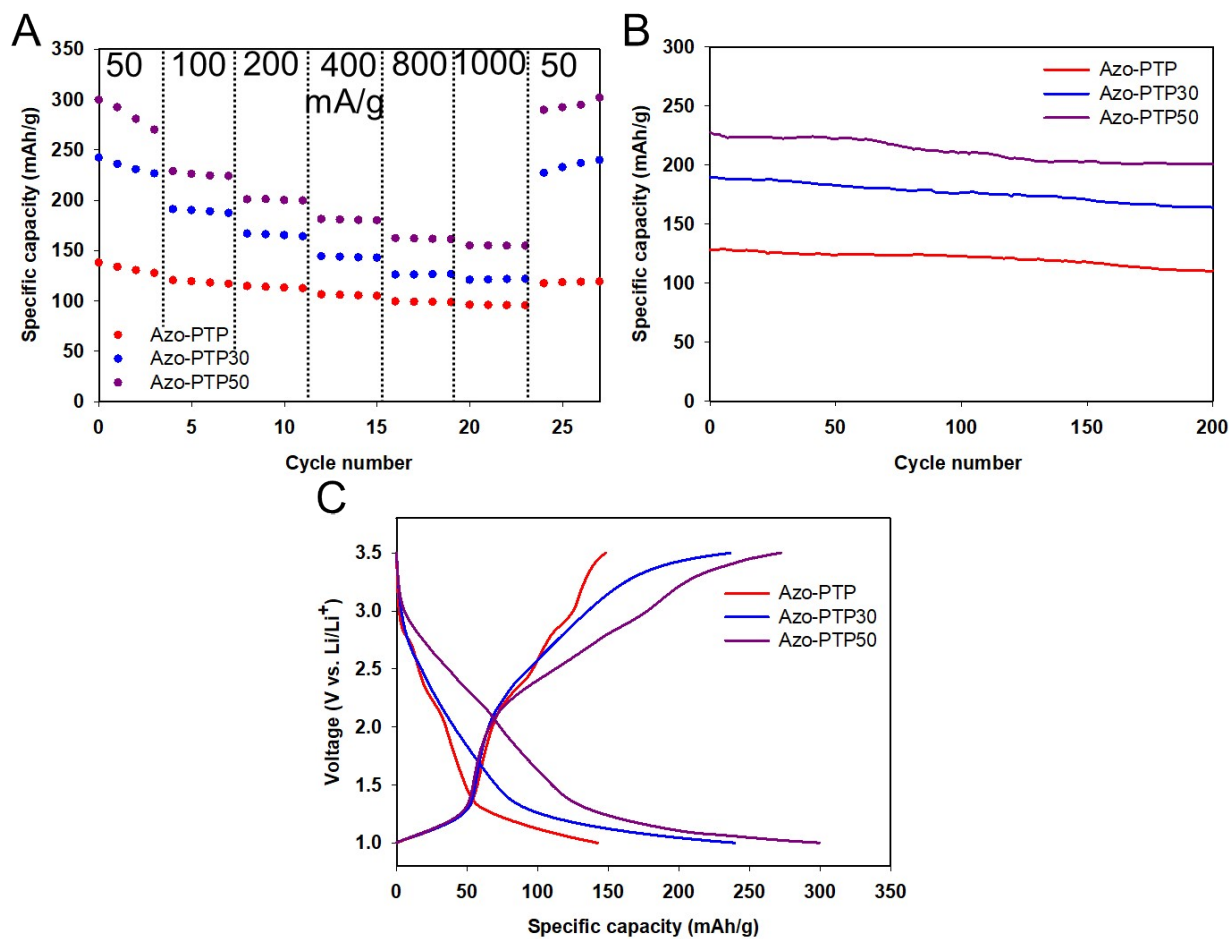


**Figure S16:** (A) Rate capability, (B) cycling stability at 100 mA g<sup>-1</sup>, and (C) galvanostatic charge/discharge at 50 mA g<sup>-1</sup> of Azo-PTP, Azo-PTP30, and Azo-PTP50 at 1.0 – 3.5 V.

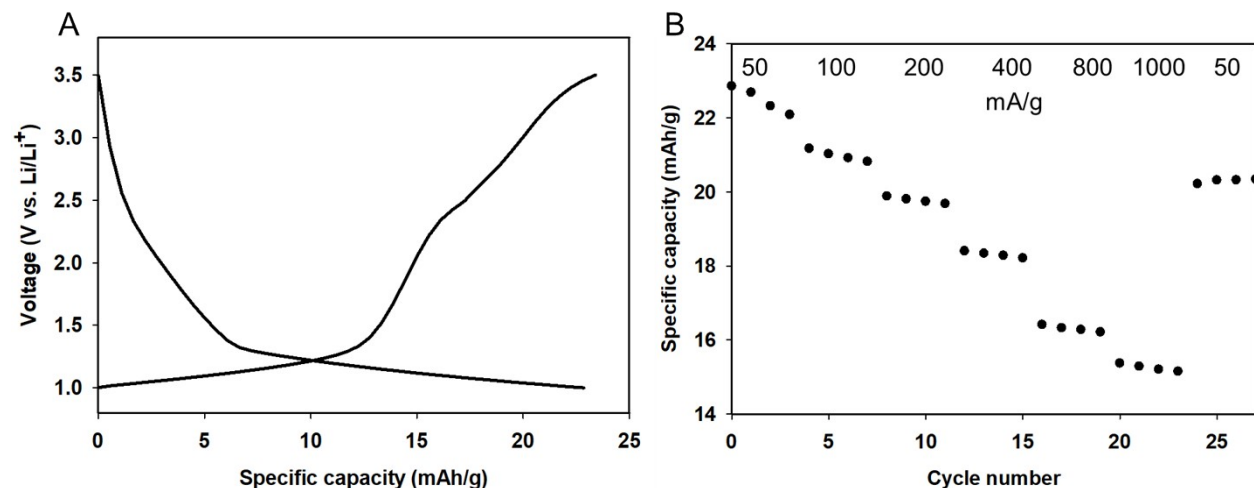


**Figure S17:** (A) Galvanostatic charge/discharge curve of CNT electrode at 50 mA g<sup>-1</sup>, (B) Rate performance of CNT electrode at 1.0 to 3.5 V.

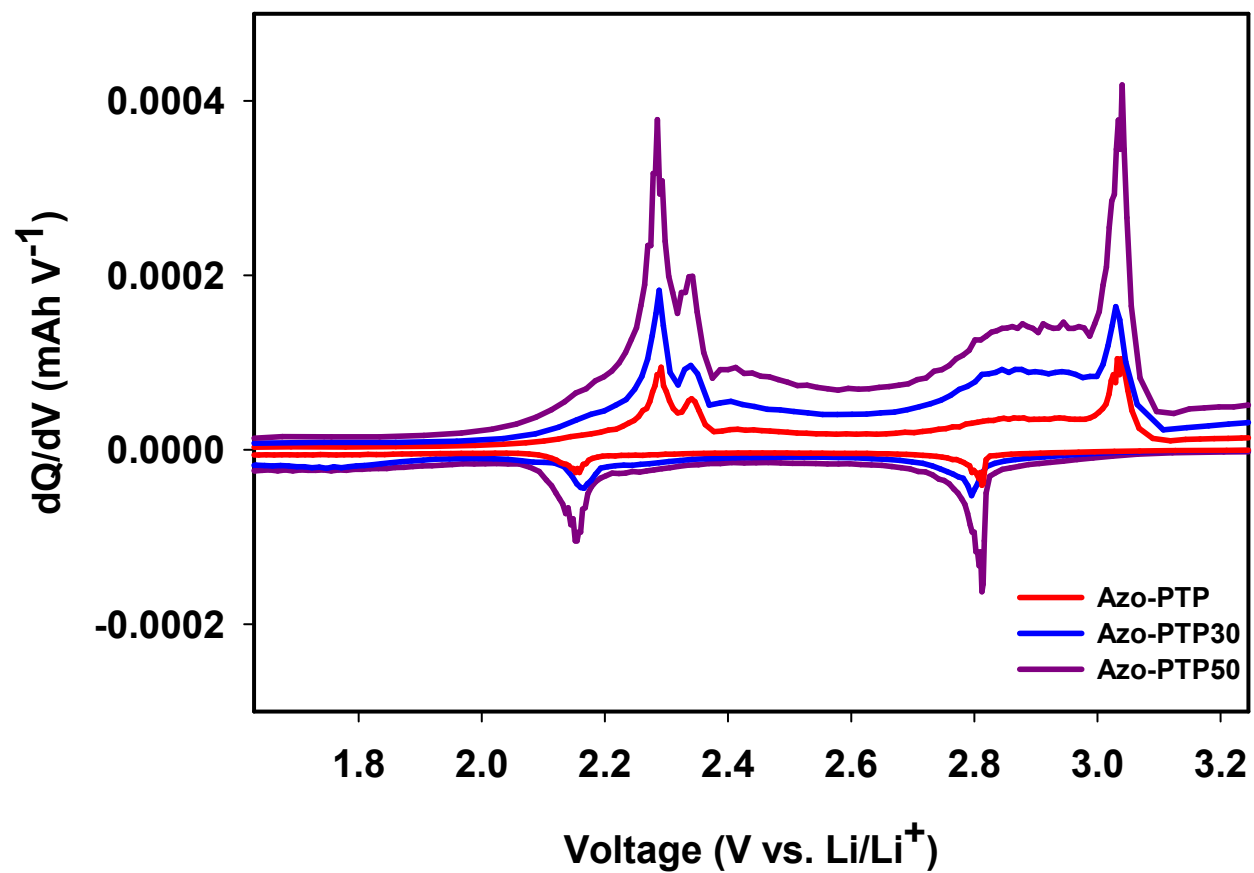


**Figure S18:** Differential capacity plots for cycle 8 of Azo-PTP (red), Azo-PTP30 (blue), and Azo-PTP50 (purple).

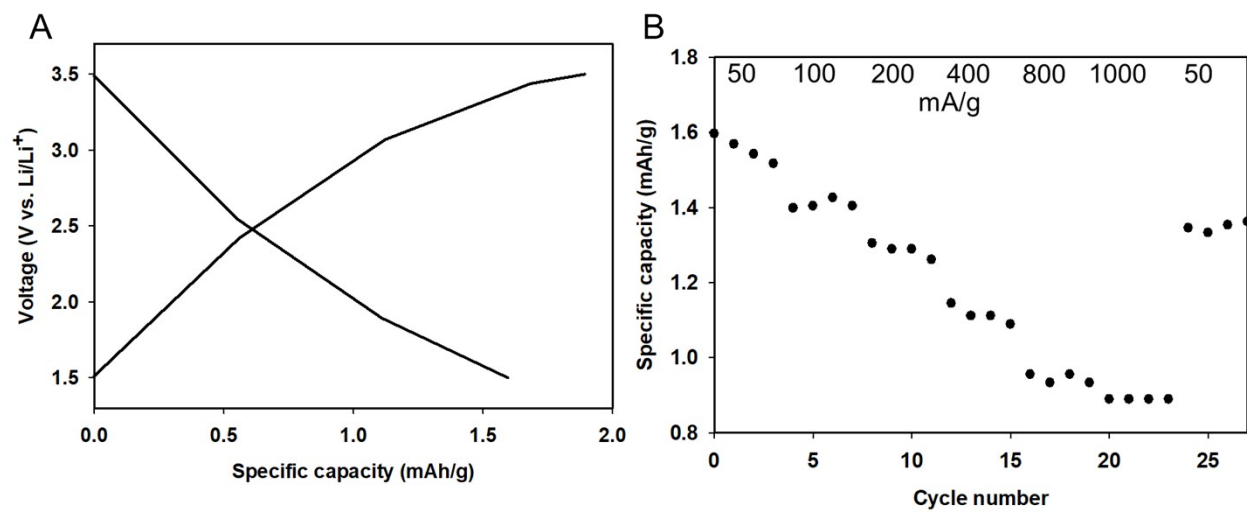


**Figure S19:** (A) Galvanostatic charge/discharge curve of CNT electrode at 50 mA g<sup>-1</sup>, (B) Rate performance of CNT electrode at 1.5 – 3.5 V.

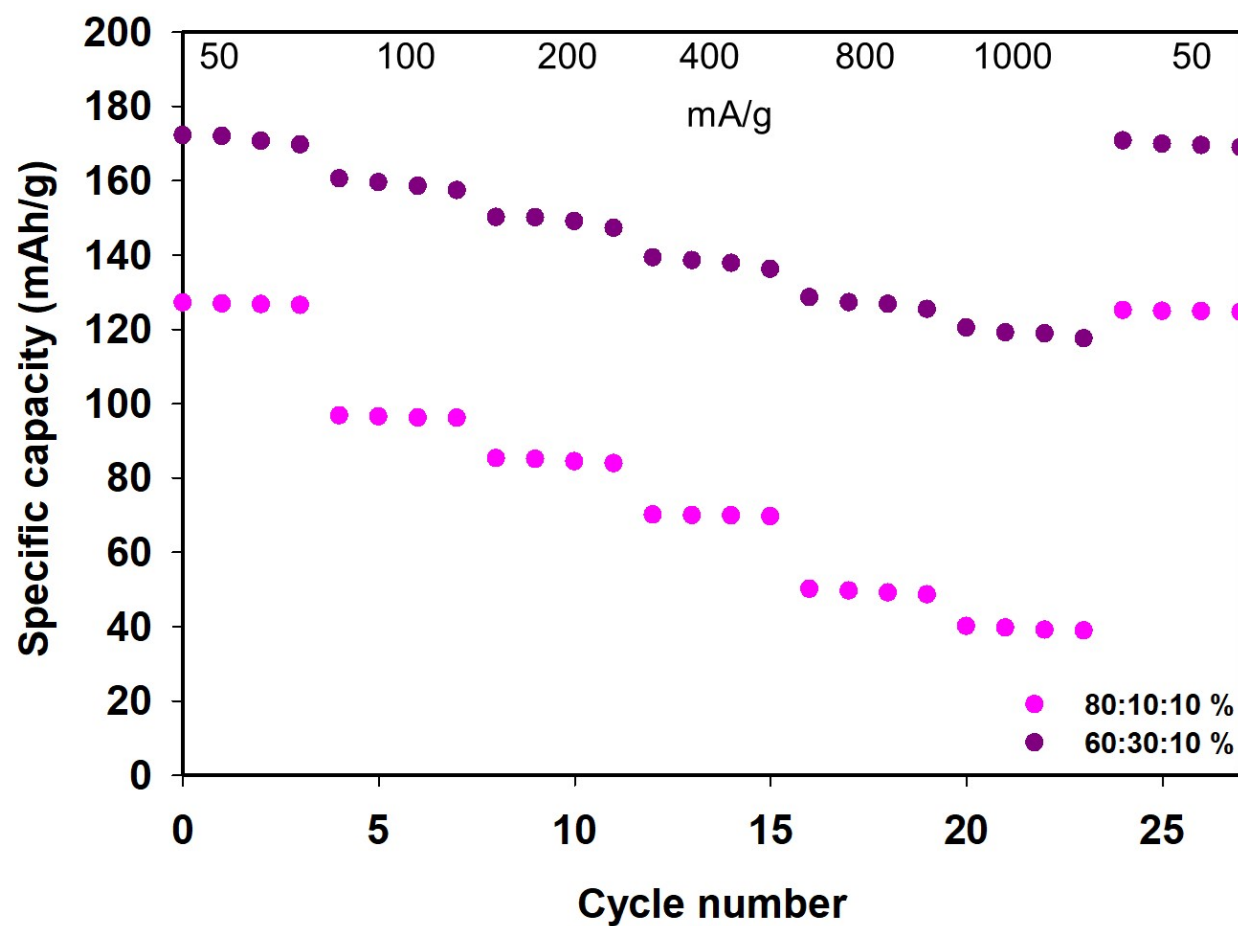


**Figure S20:** Rate capability of Azo-PTP50 electrode with two different compositions: 80:10:10 (active material: super P: PVDF, pink) and 60:30:10 (purple).

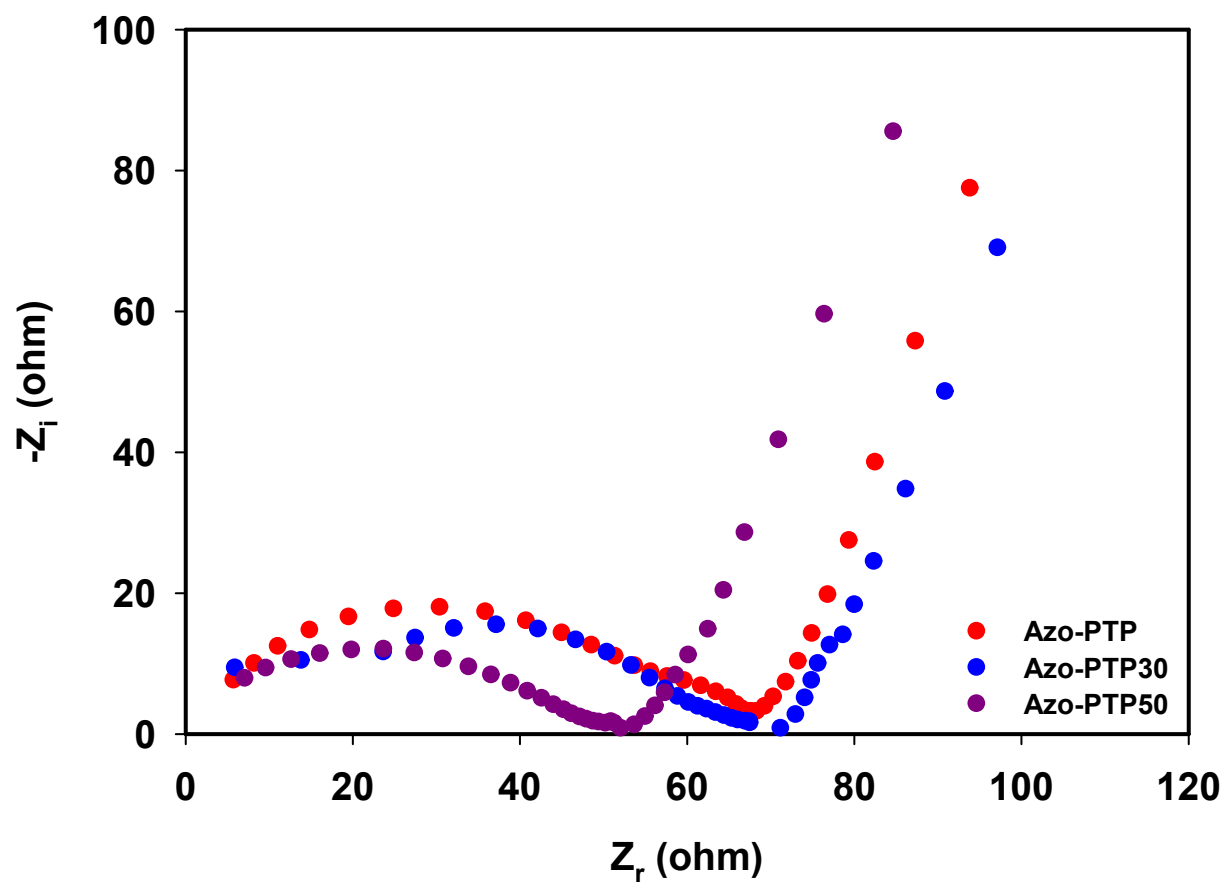


**Figure S21:** Nyquist plots of the polymers at open-circuit voltage after ten activation cycles.

**Table S2:** Summary of the specific capacity of each prepared electrodes at different current density at 1.0 – 3.5 V.

Current density (mA/g)	Azo-PTP	Azo-PTP30	Azo-PTP50
Specific capacity mAh/g			
50	141	246	300
100	125	195	230
200	119	171	204
400	109	148	185
800	102	130	167
1000	99	125	159

**Table S3:** Summary of the specific capacity of each prepared electrodes at different current density at 1.5 – 3.5 V.

Current density (mA/g)	Azo-PTP	Azo-PTP30	Azo-PTP50
Specific capacity mAh/g			
50	87.5	128.6	174.4
100	77.4	108.9	163.1
200	70.2	94.6	152.4
400	63.1	82.7	142.2
800	57.1	73.2	131.0
1000	55.9	69.7	123.2

**Table S4:** Comparison of the electrochemical performance of the prepared polymers with other organic cathodes featuring carbonyl and/or azo groups as redox-active units, as reported in the literature.

Active material	Functional group	Potential range vs Li/Li <sup>+</sup> (V)	Current density (mA g <sup>-1</sup> )	Initial discharge capacity (mAh g <sup>-1</sup> )	Retention / cycle no. (mAh g <sup>-1</sup> )	Ref.
Azo-PTP50	C=O N=N	1.0 – 3.5	50	300	89% / 200 (100)	This work
Azo-PTP30	C=O N=N	1.0 – 3.5	50	246	87% / 200 (100)	
Azo-PTP	C=O N=N	1.0 – 3.5	50	141	86% / 200 (100)	
Azo-PTP50	C=O	1.5 – 3.5	50	174	93% / 1000 (100)	
Azo-PTP30	C=O	1.5 – 3.5	50	129	91% / 1000 (100)	
Azo-PTP	C=O	1.5 – 3.5	50	88	80% / 1000 (100)	
PBALS	N=N C=O	1.0 – 3	100 = 0.5 C	220	81% / 100 (0.5 C)	7
PT-2NO <sub>2</sub>	N=N C=O	1.0 – 3.5	50	301	51% / 120 (50)	3
NHP	N=N	1.0 – 3.5	50	80	13% / 160 (50)	6
NHP@CNT-3	N=N	1.0 – 3.5	50	120	63% / 160 (50)	
PAH	N=N	1.0 – 3.5	100	254	61% / 200 (100)	8
AZO-HATN-AQ	C=O N=N C=N	1.0 – 4.0	50	240	83% / 2000 (2000)	9
D-PTO	C=O	1.5 – 4.0	100	137	68% / 50 (100)	10
PT-COF50	C=O	1.5 – 3.5	200	280	82% / 3000 (2000)	4
PT-COF	C=O	1.5 – 3.5	200	193	99% / 150 (200)	

### 3 References

- 1 J. A. Letizia, S. Cronin, R. P. Ortiz, A. Facchetti, M. A. Ratner and T. J. Marks, *Chemistry A European J*, 2010, **16**, 1911–1928.
- 2 T. Nokami, T. Matsuo, Y. Inatomi, N. Hojo, T. Tsukagoshi, H. Yoshizawa, A. Shimizu, H. Kuramoto, K. Komae, H. Tsuyama and J. Yoshida, *J. Am. Chem. Soc.*, 2012, **134**, 19694–19700.
- 3 Q. Li, H. Wang, H. Wang, Z. Si, C. Li and J. Bai, *ChemSusChem*, 2020, **13**, 2449–2456.
- 4 H. Gao, A. R. Neale, Q. Zhu, M. Bahri, X. Wang, H. Yang, Y. Xu, R. Clowes, N. D. Browning, M. A. Little, L. J. Hardwick and A. I. Cooper, *J. Am. Chem. Soc.*, 2022, **144**, 9434–9442.
- 5 P. Arab, E. Parrish, T. İslamoğlu and H. M. El-Kaderi, *J. Mater. Chem. A*, 2015, **3**, 20586–20594.
- 6 X. Ma, Y. Dong, C. He, N. Jiang and Y. Yang, *Mater. Adv.*, 2022, **3**, 5818–5825.
- 7 C. Luo, X. Ji, S. Hou, N. Eidson, X. Fan, Y. Liang, T. Deng, J. Jiang and C. Wang, *Advanced Materials*, 2018, **30**, 1706498.
- 8 Z. Sun, H. Liu, M. Shu, Z. Lin, B. Liu, Y. Li, J. Li, T. Yu, H. Yao, S. Zhu and S. Guan, *ACS Appl. Mater. Interfaces*, 2022, **14**, 36700–36710.
- 9 Z. Sun, H. Yao, J. Li, B. Liu, Z. Lin, M. Shu, H. Liu, S. Zhu and S. Guan, *ACS Appl. Mater. Interfaces*, 2023, **15**, 42603–42610.
- 10 L. Ueberricke, F. Mildner, Y. Wu, E. Thauer, T. Wickenhäuser, W.-S. Zhang, Y. Vaynzof, S. M. Elbert, R. R. Schröder, R. Klingeler and M. Mastalerz, *Mater. Adv.*, 2023, **4**, 1604–1611.